

## Recent results from the Yakutsk array experiment

V.P. Egorova, A.V. Glushkov, A.A. Ivanov \*, S.P. Knurenko, V.A. Kolosov, A.D. Krasilnikov,  
 M.I. Pravdin and I.Ye. Sleptsov

*Institute of Cosmophysical Research and Aeronomy, Yakutsk 677891, Russia*

Recent experimental results on ultra-high energy cosmic rays (UHECR) from the Yakutsk array are reported

KEYWORDS: Cosmic ray, extensive air shower, Yakutsk array

### §1. Introduction: present status of the array

The first observational period of the Yakutsk array started in 1970 with 13 scintillator and air Cherenkov light detectors covering  $\sim 3 \text{ km}^2$  area.<sup>1)</sup> In 1973 was completed so-called 'the first stage array' consisting of 35 stations ( $2 \times 2 \text{ m}^2$  scintillators and photomultiplier tubes (PMT)),  $S \sim 17 \text{ km}^2$ . During the period after 1976 the different area muon detectors were constructed. The second stage configuration was formed to 1991 when 18 stations were added with 0.5 km spacing in the inner part of the array but 10 outer stations were removed so the actual area is  $\sim 10 \text{ km}^2$ .

In the central part, the 'autonomous' sub-array is organized last years in order to study the air Cherenkov light in the energy range  $10^{15} - 10^{17} \text{ eV}$ , consisting of 14 PMTs with independent trigger.<sup>2)</sup> Inter-detector distances of PMTs are 50, 100, 200 m., the sub-array area is  $\sim 3 \text{ km}^2$ . A schematic plan of the array is shown in Fig. 1.

In Table I the average annual number of showers in the energy intervals are shown. The array is switched off during four summer months, in average. Muon detectors ( $E \geq 1 \text{ GeV}$ ) are working in  $\sim 70\%$  of events. Air Cherenkov light detectors are working in  $\sim 8\%$  of events.

Table I. Average number of events detected during 8 months

Energy	n
$> 10^{17} \text{ eV}$	60000
$> 10^{18} \text{ eV}$	2000
$> 10^{19} \text{ eV}$	10-15

### §2. Shower structure measurements

Below are given some results of our measurements concerning shower structure parameters. Lateral density distribution function (LDF) of electrons and muons are detected with scintillation counters of the array. In Fig. 2 the experimental and model simulation results are com-

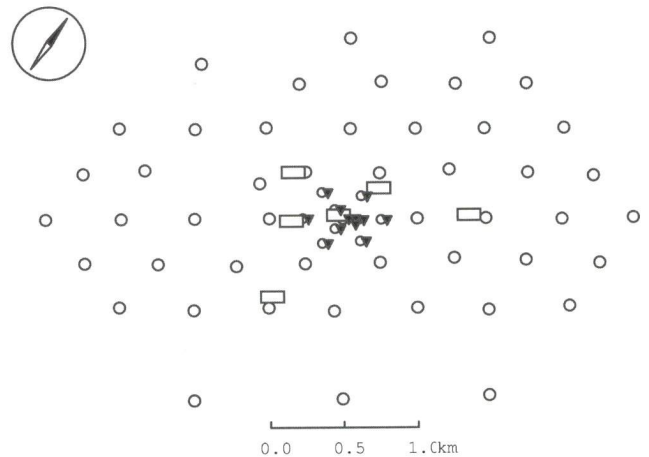


Fig. 1. Detector arrangement of the Yakutsk array. The main detectors are shown: scintillation counters+PMTs on the ground (circles), underground scintillation counters (rectangles), PMTs of autonomous sub-array (triangles).

pared for inclined showers at  $8 \times 10^{17} \text{ eV}$  and  $1.8 \times 10^{19} \text{ eV}$ . At higher energy there is seen a discrepancy between the measured muon content and expected one for the model used: although the QGSjet<sup>3)</sup> model result only is shown here, we insist that other conventional models also branch out of experiment above  $10^{19} \text{ eV}$ .

An example of lateral spread of Cherenkov photons measured with autonomous sub-array is shown in Fig. 3.

We are using the LDF slope of Cherenkov photons at different distances from the shower core to estimate the average shower maximum depth in the atmosphere,  $X_{max}$ .<sup>4)</sup> In Fig. 4 our experimental results are shown together with model simulations for the primary protons and nuclei. A tendency is indicated towards heavier composition above the knee, and proton-dominated primary composition at the highest energies as was stated before.<sup>4)</sup>

\* Presenting author, e-mail: a.a.ivanov@ikfia.ysn.ru

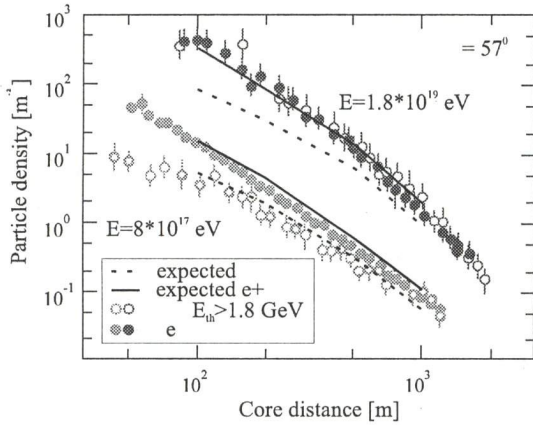


Fig. 2. Lateral distribution of charged particles and muons. Measurement results are shown by: open circles ( $\mu$ ), black and grey circles ( $e + \mu$ ). Model simulations: full curve - expected LDF of  $e + \mu$ ; dotted curve - expected LDF of  $\mu$

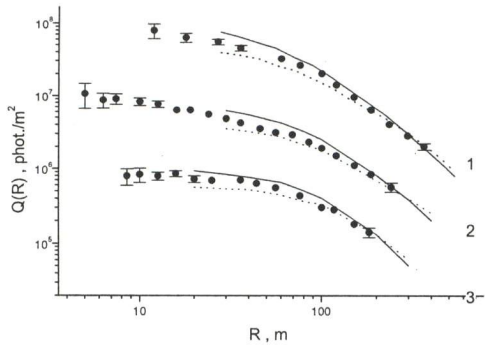


Fig. 3. Lateral distribution of Cherenkov photons. Captions: circles - measured densities at  $10^{15}$  (3),  $10^{16}$  (2),  $10^{17}$  eV (1) with statistical uncertainties shown by vertical bars. Dotted curves - calculation results for primary iron nuclei, and solid curves - for primary protons.

Attenuation curves of the particle density can be measured in inclined showers with given intensity defined by the primary energy. In such a procedure the equi-intensity cuts of spectra at different zenith angles are made in order to derive the zenith angle dependence of the measured  $S_{600}$ , particle density at 600 m from the core. The equi-intensity curves of the Yakutsk array data are shown in Fig. 5 as a function of  $X = 1020/\cos(\theta)$ . We have two distinctive areas: below and above  $\theta \sim 50^\circ$  where  $S_{600}$  attenuation lengths are significantly different. This is experimental evidence of the muon content at 600 m from the core appearing considerable above zenith angle indicated.

At  $\theta \leq 50^\circ$  where the muon content is negligible these cuts approximate the cascade curve of shower electrons. On the contrary, in inclined showers with considerable muon content, the cuts differ from the cascade curve of muonic component because of the charged pion/kaon decay rate in the atmosphere depending on zenith angle.

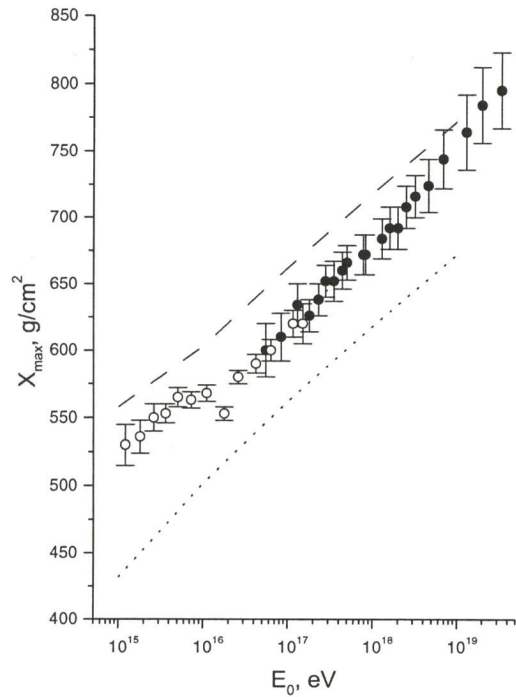


Fig. 4.  $X_{max}$  reconstructed from air Cherenkov light measurements. Open circles give autonomous sub-array results, while black circles - from the main array. QGSjet model simulation results are plotted by the dashed curve for primary protons and by dots for nuclei.

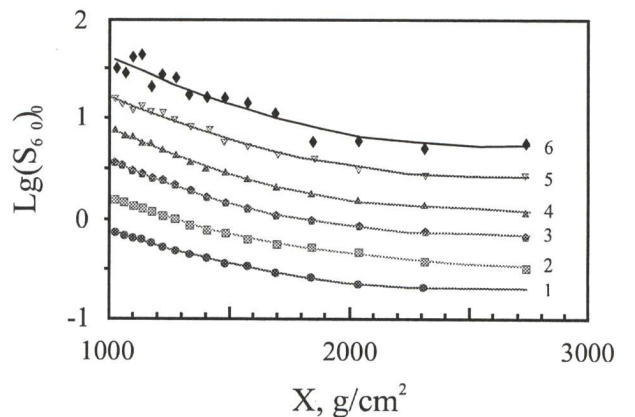


Fig. 5. Equi-intensity curves of the particle density at 600 m from the shower core. Numbers near the smoothed curves approximating experimental points indicate the fixed intensities in arbitrary units.

### §3. Energy spectrum

To illustrate the measurement results obtained with an autonomous Cherenkov sub-array we present here the energy spectrum of cosmic rays in the range  $10^{15} - 4 \times$

$10^{17}eV$  (Fig. 6). The main feature of the spectrum is a 'knee' at the energy  $\sim 4 \times 10^{15}eV$ , just where it should be according to a number of previous measurements.

Fig. 7 shows the energy spectrum at highest energies

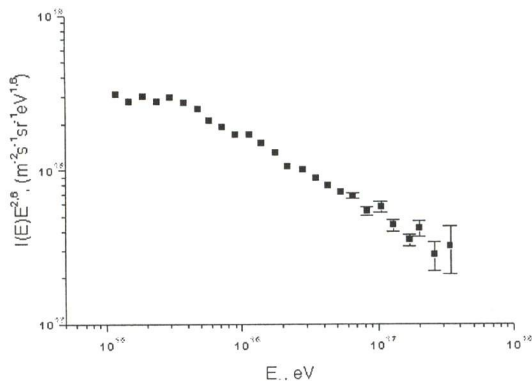


Fig. 6. CR energy spectrum from air Cherenkov light measurement

measured with scintillator detectors of the Yakutsk array together with recent spectra of AGASA<sup>5)</sup> (rectangles, 3) and the Fly's Eye<sup>6)</sup> arrays (crosses, 4). Our data set, updated in comparison with that used in Salt Lake City paper,<sup>7)</sup> is divided into two parts:

i) showers detected with stations spaced 500 m from each other (trigger-500, circles, 1) collected in the area  $2.5 \text{ km}^2$  (period 1979-1992) and  $7.2 \text{ km}^2$  (1992-1998),  $\theta < 45^\circ$ ,  $ST\Omega = 2.2 \times 10^{15} m^2 s sr$ . In each shower the charged particle density at 300 m from the core,  $S_{300}(\theta = 0^\circ)$ , is derived which in turn is used to estimate the primary energy:

$$E_0 = (5.87 \pm 1.23) \times 10^{16} \times S_{300}(\theta = 0^\circ)^{0.96 \pm 0.02}$$

$$\lambda_{300} = (288 \pm 18) + (60 \pm 7) \log(E_0/10^{18})$$

$$+ (191 \pm 12)(\sec\theta - 1).$$

ii) showers detected with stations spaced 1000 m from each other (trigger-1000, triangles, 2) collected in the area  $25.8 \text{ km}^2$  (period 1974-1990) and  $16.6 \text{ km}^2$  (1990-2000),  $\theta < 60^\circ$ ,  $ST\Omega = 2.6 \times 10^{16} m^2 s sr$ . Data collection area was extended in these cases outside of an array domain in order to increase the number of events. In each shower the charged particle density at 600 m from the core,  $S_{600}(\theta = 0^\circ)$ , is derived which is used to estimate the primary energy:

$$E_0 = 4.8 \times 10^{17} \times S_{600}(\theta = 0^\circ)$$

$$\lambda_{600} = 460 + 32 \log(E_0/10^{18}), \theta < 50^\circ$$

$$\lambda_{600} = 1000, 50^\circ < \theta < 60^\circ.$$

An updated spectrum exhibits the same features: some kind of an 'ankle' around  $\sim 10^{19}eV$  and a lack of showers

above  $\sim 10^{20}eV$  relative to AGASA result, although the sample size of the Yakutsk array data is insufficient yet to be undoubted.

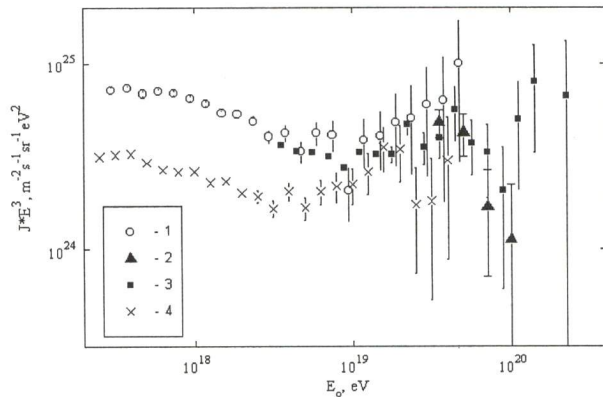


Fig. 7. Energy spectrum of primary cosmic rays. Figure captions are explained in the text.

#### §4. Arrival directions

An actual topic of investigations is arising due to recently found indications of an excess flux of cosmic rays from the galactic plane regions at the highest energies: center<sup>8)</sup> ( $E = 10^{18}eV$ ), plane<sup>9)</sup> ( $E < 3.2 \times 10^{18}eV$ ), and north-south asymmetry<sup>10)</sup> ( $E = 10^{19}eV$ ).

Arrival direction distribution of the Yakutsk array updated data set is studied using harmonic analysis (Fig. 8), asymmetry parameters (Fig. 9) and time series (Fig. 10). While the first three harmonics don't reveal any strong deviation from the isotropic expectation, we have a significant north-south asymmetry in galactic latitudes at ( $E = 10^{19}eV$ ). The details of the method used are given in the previous paper.<sup>10)</sup> If to attribute the observed southern excess to galactic nuclei ( $Z \sim 10$ ) originating in the disk, the result is in qualitative agreement with that of AGASA<sup>8)</sup> and the Fly's Eye<sup>9)</sup> arrays because of the same rigidity of supposed primaries causing effects. Harmonic analysis doesn't reveal the proposed extra flux from the galactic center due to the Yakutsk array acceptance area outside this region.

We have analyzed the time series of the Yakutsk array data in four energy intervals in order to check - is there any inhomogeneity in a temporal spread of the cosmic ray intensity<sup>12)</sup> (Fig. 10). Low energy intervals show intensities which can be well described by the constant. On the contrary, the intensity of highest energy showers at  $E \geq 10^{19}eV$  seems steadily declining linearly

$$\Delta J / \Delta T = -0.008 \pm 0.004 \text{ per year.}$$

The variations of the observed intensity caused by the array operation conditions or by the data sampling/processing methods were ruled out.

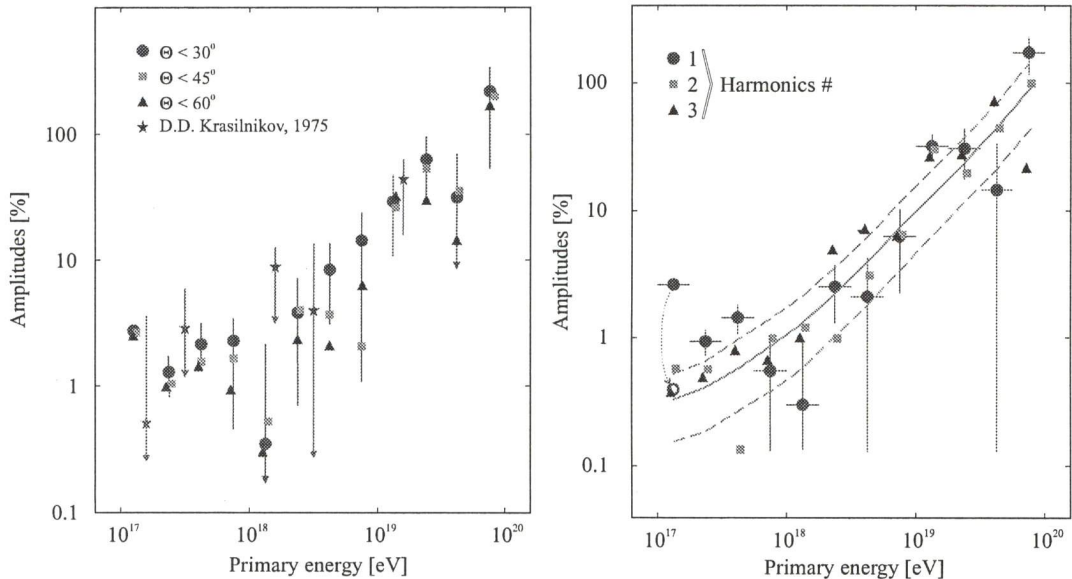


Fig. 8. The left panel: observed amplitudes in three zenith intervals. Early results of the Haverah Park, Sydney and Yakutsk arrays summarized by Krasilnikov<sup>11)</sup> are given for comparison. The right panel: the first three harmonics (points) and expected-for-isotropy amplitudes (solid curve) with rms deviations (dashed curves). The very left shifted point illustrates a correction for seasonal and diurnal variations of the array acceptance.

### §5. Azimuthal asymmetry

Giant ground arrays like Yakutsk, AGASA etc. cannot measure the total number of particles reaching the surface; the density at fixed distance from the axis,  $S_{600}/S_{300}$  is used to parameterize the showers instead. This leads to geomagnetic effect on the average charged particle density which depends on the arrival direction of a shower in regard to magnetic field vector.

Due to a few detectors fired in particular showers, especially at lower energies, it is difficult to analyze the oval lateral distribution of particles. It is more convenient to count the event rate of showers with fixed  $S_{300}$  and zenith angle at different azimuths. In this case the primary energy and intensity (due to rapidly falling spectrum) are functions of azimuth.

The Yakutsk array data at  $E > 5 \times 10^{16} eV$  have the pronounced azimuthal effect on the charged particle density as was shown earlier<sup>13)</sup> (Fig. 11).

Owing to the dip angle of the magnetic field in Yakutsk ( $14^\circ$ ) the first harmonic amplitude is predominant here. The second harmonic should be a majorant for equatorial arrays. The magnitude of the measured effect is small for vertical showers but is firmly increasing with zenith angle (Fig. 12).

The azimuthal effect should be taken into account in the primary energy estimation/EAS size spectrum measurement in inclined events, and corrections should be

made to arrival direction distribution plotted in the declination or galactic coordinates. In order to illustrate the influence of the geomagnetic effect on arrival directions in galactic coordinates we have calculated the ratio of observed and expected-for-isotropy distributions (Fig. 13). An 'observed' distribution was derived using zenith and azimuth angles of real showers but uniform sidereal time distribution. In the case of 'isotropic' expectation a uniform spread in azimuth was used instead of experimental one. At higher energies ( $E > 2 \times 10^{18} eV$ ) the statistical accuracy of the Yakutsk array data is insufficient to reveal the distribution non-uniformity. But in the energy range  $E > 10^{17} eV$  there is a clear systematic effect of the magnitude  $\sim 10\%$ .

### §6. Conclusion

We have summarized the series of recent results from the Yakutsk array showing the present status and actual evolution of the array towards the methodical instrument aimed to the energy region  $10^{15} < E < 10^{20} eV$ . Multi-parameter measurements realized here form an experimental basis for planned giant arrays of the next generation.

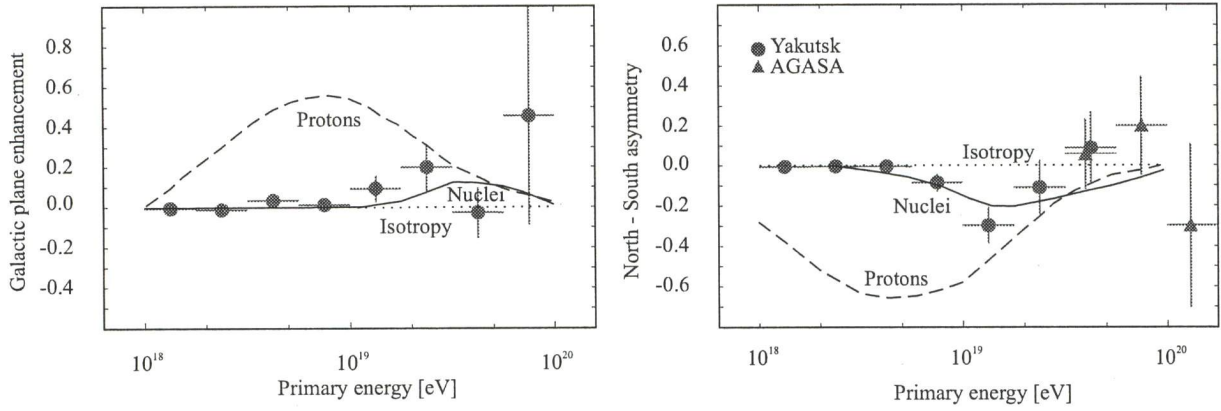


Fig. 9. The left panel: galactic plane enhancement. The right panel: the north-south asymmetry. Experimental points of the Yakutsk and AGASA arrays are shown with statistical errors (vertical bars) and energy bins (horizontal bars). The curves are model calculation results for galactic protons and nuclei ( $Z \sim 10$ ) admixed to the isotropic extra-galactic CRs.

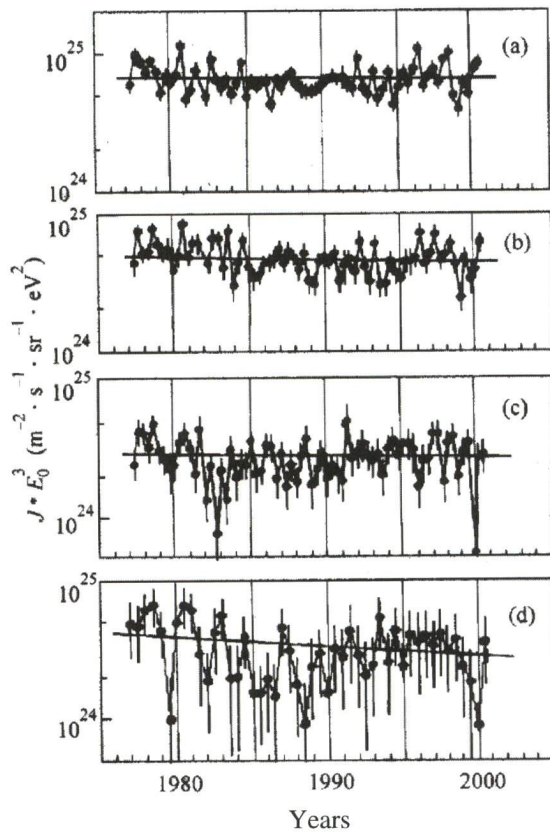


Fig. 10. Temporal spread of the intensity of cosmic rays. Points are experimental data and the straight lines are their linear approximations in the energy intervals: (a)  $E < 10^{18}$  eV (6684 showers), (b)  $10^{18} \leq E < 3 \times 10^{18}$  eV (3253 showers), (c)  $3 \times 10^{18} \leq E < 10^{19}$  eV (1331 showers), and (d)  $E \geq 10^{19}$  eV (214 showers).

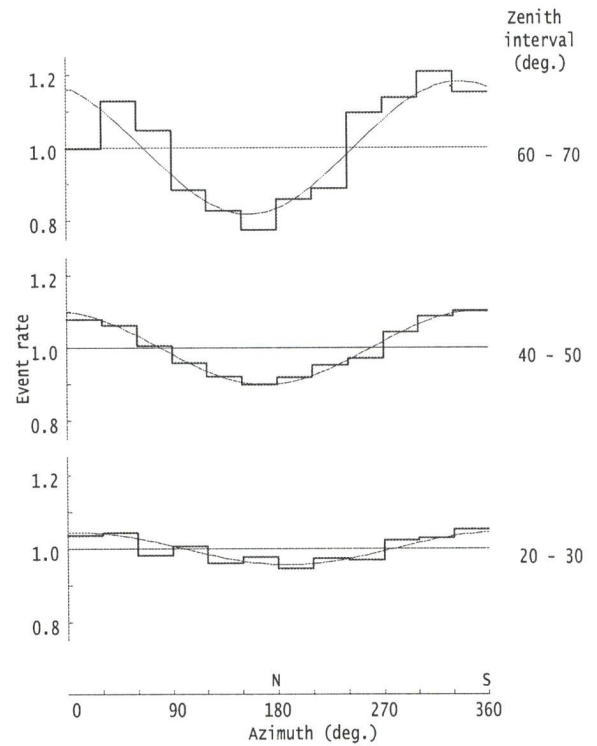


Fig. 11. Azimuthal effect on the charged particle density. Zenith angle intervals are indicated on the right side. Experimental data are shown by histograms while the dashed curves are the first harmonic approximations.

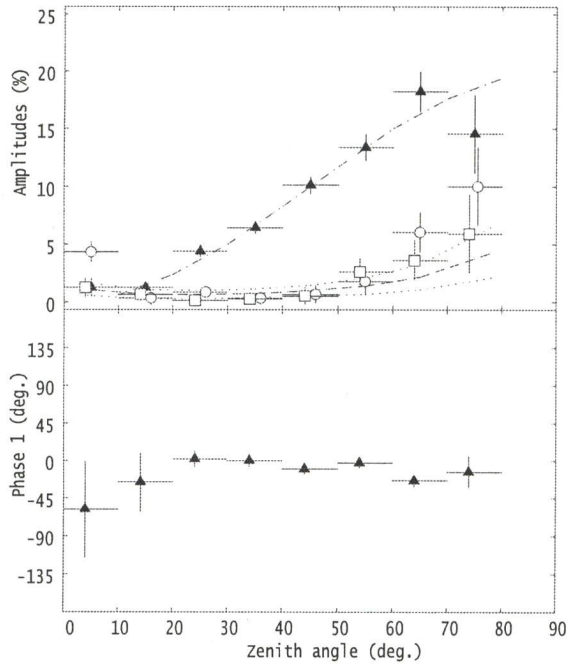


Fig. 12. Amplitudes of three harmonics and a phase of the first harmonic. Measured amplitudes are shown by: triangles (first), circles (second), rectangles (third harmonics). The dash-n-dot curve shows  $0.2\sin^2\theta$  approximation. Expected for uniform distribution amplitudes for all harmonics are shown by the dashed curve, with r.m.s. variations shown by the dots.

### Acknowledgements

This work is supported by RFBR (grants n.00-07-90161, n.01-02-17281) and Ministry of Sciences of Russia (grant n.01-30). AAI would like to acknowledge Professor M. Teshima and AGASA team for invitation and hospitality during the Workshop and for the financial support for a visit to Japan.

- 1) T.A. Egorov, N.N. Efimov, V.A. Kolosov *et al.*: 12th ICRC **6** (Hobart, 1971) 2059.
- 2) B.N. Afanasiev, S.P. Knurenko, V.A. Kolosov *et al.*: 25th ICRC **7** (Durban, 1986) 217. 96. 94.
- 3) A.V. Glushkov, M.I. Pravdin, V.R. Sleptsova *et al.*: 26th ICRC **1** (Salt Lake City, 1999) 399.
- 4) M.N. Dyakonov *et al.*: 23th ICRC **4** (Calgary, 1993) 303.
- 5) M. Takeda *et al.*: 26th ICRC **3** (Salt Lake City, 1999) 3 252.
- 6) O.J. Bird *et al.*: *Astroph. Journ.* **424** (1994) 491.
- 7) M.I. Pravdin *et al.*: 26th ICRC **3** (Salt Lake City, 1999) 292.
- 8) N. Hayashida *et al.*: *Astropart. Phys.* **10** (1999) 303.
- 9) D.J. Bird *et al.*: astro-ph/9806096 (1998).
- 10) A.A. Ivanov: *J. Phys. G.* **24** (1998) 227.
- 11) D.D. Krasilnikov: *Issled. Kosmofiz. i Aeron.* (Yakutsk, 1975) 69.
- 12) A.V. Glushkov and M.I. Pravdin: *JETP lett.* **73** (2001) 131.
- 13) A.A. Ivanov *et al.*: *JETP Lett.* **69** (1999) 288.

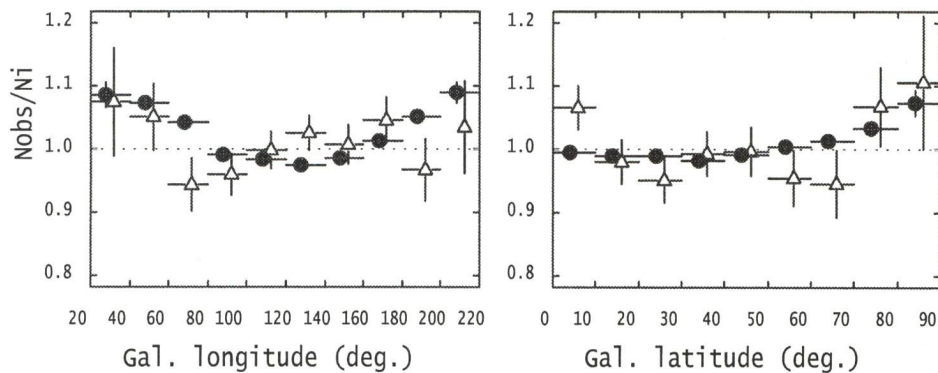


Fig. 13. The ratio of observed (Nobs) to isotropic (Ni) numbers of showers in galactic coordinates. Two data sets are used:  $E > 10^{17}eV$  (circles) and  $E > 2 \times 10^{18}eV$  (triangles).